

# CLASSIFIED-FILTER-BASED POST-COMPENSATION INTERPOLATION FOR COLOR FILTER ARRAY DEMOSAICING

<sup>1</sup>Jing-Ming Guo, *Senior Member, IEEE*, <sup>1</sup>Yun-Fu Liu, *Student Member, IEEE*, <sup>1</sup>Bo-Syun Lai, <sup>2</sup>Peng-Hua Wang, and <sup>3</sup>Jiann-Der Lee, *Member, IEEE*

<sup>1</sup>Department of Electrical Engineering,  
National Taiwan University of Science  
and Technology,  
Taipei, Taiwan

<sup>2</sup>Department of Computer Science and  
Information Engineering,  
National Taipei University,  
Taipei, Taiwan

<sup>3</sup>Department of Electrical Engineering,  
Chang Gung University,  
Taoyuan, Taiwan

E-mail: [jmguo@seed.net.tw](mailto:jmguo@seed.net.tw), [yunfuliu@gmail.com](mailto:yunfuliu@gmail.com), [m9907314@mail.ntust.edu.tw](mailto:m9907314@mail.ntust.edu.tw), [phwan@mail.ntpu.edu.tw](mailto:phwan@mail.ntpu.edu.tw), [jdlee@mail.cgu.edu.tw](mailto:jdlee@mail.cgu.edu.tw)

**Abstract**—In this paper, a classified-based post-compensation algorithm for Color Filter Array (CFA) demosaicing is proposed. This technique can be used for improving the image quality of the interpolated results obtained by other CFA images. First, each pixel is classified according to its neighborhood texture variance and angle. Then, different Least-Mean-Square (LMS) filters are trained to adopt for dealing pixels of various characteristics. As documented in the experimental results, the proposed scheme can substantially boost the image quality; in addition, a better visual perceptual can be obtained. Notably, the proposed method can be considered as effective post-compensation by applying for any former schemes to yield an even better image quality.

**Keywords:** *Color filter array, least mean squares, demosaicing, color interpolation, Bayer pattern.*

## 1. INTRODUCTION

Nowadays, more and more people take photos by digital cameras instead of traditional analog film models. To capture digital image data, various types of sensor systems were designed, such as field sequential, multi-chip, Foveon X3, and Color Filter Array (CFA). Among them, field sequential relied on a disc of color filters inside the receiver, capturing colors in sequence, yet it may cause color breakup phenomena. Multi-chip utilizes a prism to refract green, red and blue lights based on the wavelength characteristics to three different Charge Coupled Devices (CCDs). Foveon X3 sensor also takes advantage of the wavelength characteristics of light to detect information by multilayer sensor at each absorption level. Nevertheless, the majority of digital cameras favor the CFA as sensor array to reduce the cost, and the most prevalent array is the Bayer CFA [1]. The green color is recorded twice than that of the red or blue color since the Human Visual System (HVS) is more sensitive to the green spectrum. Because each pixel location saves only one color in CFA, the other two missing color values are obtained through an estimation procedure, namely, interpolation or demosaicing.

Bilinear Interpolation (BI) [2] is the simplest method, which only computed the missing values from the average of its neighbors. Although BI can provide satisfactory results in low frequency regions of an image, it always produces wrong results in high frequency regions. The reason it induces artifacts (such as zippers, Moiré pattern and blurring artifacts) on high frequency part can be blamed that it simply considers the neighboring pixels without directional information. For instance, this method may interpolate across an edge, and the recovered edge will be distorted. Thus, many interpolation techniques have been proposed

in recent years to overcome these problems. Some algorithms introduced Edge-Directed Interpolation (EDI) which analyzed the region around each pixel to determine interpolation direction, and then interpolated according to the direction. For example, Adaptive Color Plane Interpolation (ACPI) [3] performed a vertical and horizontal gradient test, afterward the interpolation was applied along the direction of a small gradient to determine the missing pixel. The algorithm proposed in [4] improved the decision making process of edge direction using variance of color differences as a supplementary criterion. The other group of common ways in demosaicing is based the assumption that the hue is locally constant. The constant-hue-based method first interpolated the green channel by bilinear or EDI, then used the color ratio between green and red (blue) to estimate the blue (red) channel [5], [6]. The scheme in [7] employed the mathematical model such as Taylor series and cubic spline, the estimable values were interpolated in four opposite directions, and then applied classifier and median filter to determine the best value. After that, they improved their method using a weighted median filter. Its coefficients were determined by a classifier which based on an edge orientation map. Although the above methods can produce good results for different types of image, there are, however, rooms for improving image quality. Thus, a post-compensation scheme is proposed to further enhance the image outcomes of CFA. In this paper, based upon on the framework, namely High-Order Interpolation with Weighted Median filter (WM-HOI) [8], which provides good image quality without recursive procedure, the proposed post-compensation algorithm with adaptive filtering strategy is proved to further improve the image quality. Three parts are involved in the proposed scheme: 1) A classifier is used to determine the category group of each pixel according to its local angle and variance; 2) the Least-Mean-Square (LMS) algorithm [9], [10] is used to adjust and train the coefficients of each filter based on the classified result from part one; 3) the optimized filters are then used to generate the corresponding output images.

The rest of this paper is organized as below. The proposed Classified-Filter-based Post-Compensation Interpolation (CF-PCI) algorithm for CFA demosaicing is undertaken in Section 2. Afterward, Section 3 demonstrates the performances of the proposed CF-PCI method in various aspects. Finally, Section 4 draws the conclusions and future works.

## 2. PROPOSED CLASSIFIED-FILTER-BASED POST-COMPENSATION INTERPOLATION METHOD

According to the observation that although the former method WM-HOI provides good image quality, it still has some room for further improvement, such as a more accurate direction decision and further consideration of the edge strength. Thus, an algorithm is proposed to classify each pixel with five different angles and two variance features, and the post-compensation filter banks are trained using the Least-Mean-Square (LMS) algorithm for demosaicing. The latter feature is used to differentiate different edge strengths; the numbers of each feature and how to select these two kinds of features are discussed in Section 4. Figure 1(a) shows the block diagrams of the proposed post-compensation schemes, including the post-compensation and off-line LMS training procedure. Firstly, a CFA image is captured from a camera with Bayer CFA, and the image is interpolated by the former WM-HOI method [8]. All of the pixels in the WM-HOI image are continually classified according to the corresponding angle and variance, and the classification map is used to store the related classified information. Based on this map, the WM-HOI image is further processed with the optimized LMS filters to yield the output images, in which the filters are obtained by the off-line training algorithm as illustrated in Fig. 1(b). The training algorithm is employed to adjust the coefficients of the filters until they meet the convergent condition.

### 2.1. Pixel classification

To enhance image quality and preserve the edge of CFA images, it is required to classify each pixel according to the angle and variance in advance, where the angle provides the direction information of each pixel, and variance describes the degree of dispersion. The values of the two features are divided into several groups in this study. To derive the two features, the Sobel edge detectors on horizontal and vertical directions are employed. The energies on horizontal and vertical directions denoted  $E_{i,j}^H$  and  $E_{i,j}^V$  at position  $(i, j)$  are defined as below:

$$E_{i,j}^H = H_{i,j} * \begin{bmatrix} -1 & 0 & 1 \\ -2 & 0 & 2 \\ -1 & 0 & 1 \end{bmatrix}, \quad (1)$$

$$E_{i,j}^V = H_{i,j} * \begin{bmatrix} 1 & 2 & 1 \\ 0 & 0 & 0 \\ -1 & -2 & -1 \end{bmatrix}, \quad (2)$$

where  $H_{i,j}$  denotes the WM-HOI image pixel value at position  $(i, j)$  and  $*$  denotes the convolution operator. The angle  $\theta_{i,j}$  is defined as

$$\theta_{i,j} = \tan^{-1} \frac{E_{i,j}^V}{E_{i,j}^H}. \quad (3)$$

The Sobel angle indicates the edge direction for each pixel. In addition, the additional variance feature as defined below is adopted for further classification.

$$\sigma_{i,j}^2 = \overline{\mu_{i,j}^2} - (\overline{\mu_{i,j}})^2, \quad (4)$$

where  $\overline{\mu_{i,j}}$  and  $\overline{\mu_{i,j}^2}$  denote the first-order moment and the second-order moment, respectively, as defined below.

$$\overline{\mu_{i,j}} = \frac{1}{M^2} \sum_{m,n \in M \times M} H_{i+m,j+n}, \quad (5)$$

$$\overline{\mu_{i,j}^2} = \frac{1}{M^2} \sum_{m,n \in M \times M} H_{i+m,j+n}^2, \quad (6)$$

where  $M \times M$  denotes the number of neighbors for estimation. In which, the obtained variance can characterize the frequency property of the corresponding region. Afterward, the obtained angles and variances are sorted and classified into numbers of A and B groups, respectively. These  $A \times B$  different subsets are stored in the classification map which contains the classified categories of the above two features for each pixel. The amount of pixels in each subset is forced to identical to each other, and the pixels in each subset have similar angle and variance.

### 2.2. Filter training scheme for post-compensation

The LMS algorithm invented by Widrow and Hoff [9], is an adaptive algorithm with the concept of the gradient-based method of steepest descent. This algorithm employs the estimations of the gradient vector from the available data, and incorporates an iterative procedure which successively corrects the weight vector towards the direction of the negative of the gradient vector which eventually leads to the minimum mean square error. Compared with algorithm such as the well-known Conjugate Gradient (CG) [13], the LMS algorithm is relatively simple, since it does not require correlation function calculation nor does it require matrix inversions. The LMS training procedure for those pixels which are classified to category  $(C)$  is described in mathematical forms as follows:

$$\hat{g}_{i,j} = \sum \sum_{(m,n) \in R} w_{m,n}^{(C)} \times H_{i+m,j+n}, \quad (7)$$

$$e_{i,j}^2 = (g_{i,j} - \hat{g}_{i,j})^2, \quad (8)$$

$$\frac{\partial e_{i,j}^2}{\partial w_{m,n}^{(C)}} = -2e_{i,j} \times H_{i+m,j+n}^{(C)}, \quad (9)$$

$$\Delta w_{m,n}^{(C)} = \begin{cases} \rho e_{i,j} H_{i+m,j+n}^{(C)}, & \text{if } \frac{\partial e_{i,j}^2}{\partial w_{m,n}^{(C)}} < 0 \\ -\rho e_{i,j} H_{i+m,j+n}^{(C)}, & \text{if } \frac{\partial e_{i,j}^2}{\partial w_{m,n}^{(C)}} > 0 \end{cases}, \quad (10)$$

$$w_{m,n}^{(C)}(k+1) = w_{m,n}^{(C)}(k) + \Delta w_{m,n}^{(C)}, \quad (11)$$

where  $(C)$  denotes the category, meaning the members of the same category should co-train its filter;  $g_{i,j}$  denotes the value at position  $(i, j)$  of the original image;  $\hat{g}_{i,j}$  denotes the predicted value at position  $(i, j)$ ;  $R$  denotes the support region of the LMS filter;  $e_{i,j}^2$  denotes the mean square error between  $g_{i,j}$  and  $\hat{g}_{i,j}$ ;  $w_{m,n}$  denotes the coefficient of the trained LMS filter;  $w_{m,n}^{(opt)}$  denotes coefficient of the optimized LMS filter;  $k$  denotes the number of iterations; the empirical  $\rho = 10^{-9}$  denotes the parameter adjusted to control the convergent speed of the LMS optimum procedure. The value of the parameter  $\rho$  is directly proportional to convergent speed. The results may be easily trapped into the local optimums when a large  $\rho$  is employed, and vice versa. The training process is terminated when

$$\sum \sum_{(m,n) \in R} |w_{m,n}^{(C)}(k+1) - w_{m,n}^{(C)}(k)| \leq T, \quad (12)$$

where  $T$  denotes the tolerance of total error of the filter coefficients between two consecutive iterations, and which is set at  $10^{-5}$  in this study. The parameter can produce a satisfactory result while reducing the training time.

### 2.3. Post-compensation

After the off-line filter sets training procedure proposed in sub-section 2.2, the three optimized post-compensation filter banks of size  $A \times B$  for each color channels (red, green, and blue) are produced. In a practical application, the classification map is obtained from the WM-HOI image as the source image to select a suited filter according to the angle and variance information. Then, the classified group  $W^{(C)}$  of  $H_{i,j}$  is applied as below for further enhancing the image quality and reducing artifacts such as blur and Zipper effect.

$$\hat{g}_{i,j} = \sum \sum_{(m,n) \in R} w_{m,n}^{(C)} \times H_{i+m,j+n}^{(C)}. \quad (13)$$

## 3. EXPERIMENTAL RESULTS

In this section, the performance of the proposed Classified-Filter-based Post-Compensation Interpolation (CF-PCI) method is demonstrated. Moreover, the widely-used public Kodak lossless true color image suite [14] is adopted for our experiments. To evaluate the image quality of the interpolated images, the Peak

Signal-to-Noise Ratio (PSNR) and the Color PSNR (CPSNR) as defined below are utilized,

$$PSNR = 10 \log_{10} \frac{255^2}{MSE}, \quad (14)$$

where

$$MSE = \sum_{j=1}^L \sum_{i=1}^W (g_{i,j} - \hat{g}_{i,j})^2 / (W \times L), \quad (15)$$

where  $g_{i,j}$  and  $\hat{g}_{i,j}$  denote the original image and the test image, respectively, and  $W \times L$  denotes the size of the image. On the other hand, the CPSNR is the average of the PSNRs of the three color channels.

To determine the suited features for interpolation, four different features are adopted for our simulation. Excepting for the angle and variance discussed in sub-section 2.1, two more features namely magnitude ( $MAG_{i,j}$ ) and maximum edge direction ( $MED_{i,j}$ ) had also been estimated. The corresponding definitions are formulated as below,

$$MAG_{i,j} = \sqrt{E_{i,j}^H{}^2 + E_{i,j}^V{}^2}, \quad (16)$$

$$MED_{i,j} = \max\left(\frac{E_{i,j}^H}{E_{i,j}^V}, \frac{E_{i,j}^V}{E_{i,j}^H}\right), \quad (17)$$

where the two variables  $E_{i,j}^H$  and  $E_{i,j}^V$  are defined in Eqs. (1)-(2). Fig. 2 shows the PSNRs obtained by with these four features, each curve is classified and trained with single feature. As it can be seen, the angle and variance are the best features which yield the best performance in terms of image quality over green plane.

Notably, because each color plane has a specific spectrum characteristic, three filter sets are applied for the three primary color planes. Thus, filters of various sizes are tested for different color channels to determine the optimal filter size. For this, the first 12 Kodak images are employed as training set, and the rest 12 Kodak images are considered as testing set. Fig. 3 shows the average image quality of the interpolated images with different filter sizes on green, red and blue planes respectively. As it can be seen, the curve achieves the highest performance with filter of size  $13 \times 13$  on green channel, while the best filter size is  $5 \times 5$  for red and blue channels. To show the effect of the variance feature, the coefficients of the filter pair in the first angle category associates to the high and low variance for green plane is shown in Fig. 4. According to the observation, simply the central  $5 \times 5$  area has higher weights, and the rest areas of the filter are with low responses. Considering the filters of size to  $13 \times 13$  in Fig. 4(a), the "flat" region of the filter (beyond the center  $5 \times 5$  region) also provides about 0.3 db improvement (41.9 to 42.2 dB) in terms of PSNR. In addition, the center coefficient of the low variance filter is smaller than that of the high variance filter, because the category with high variance normally associates to the edge region. Thus, the edge textures should be enhanced rather than averaged by its neighboring pixels. Notably, the other categories also have the same property.

Table I shows a comparison in terms of image quality between the WM-HOI and the proposed CF-PCI algorithms. Theoretically, the image quality obtained by the proposed post-compensation method should be improved, and the results prove this claim. Although the improvements over the red and blue planes are rather limited (about 0.27 dB), the PSNR in green plane is significantly improved by around 0.97 ~ 2.01 dB. Figure 5 shows the post-compensation result for commonly used fence region of the 19<sup>th</sup> Kodak test image for subjective quality comparison. It is interesting to note that the proposed scheme can yield more improvement over regions of high dynamic range than that of the low dynamic range regions. Herein, the dynamic range means the difference between maximum and minimum value in a

block such  $3 \times 3$ , Fig. 6 illustrates the improvement over various dynamic ranges on red and blue planes between the WM-HOI and the proposed CF-PCI.

#### 4. CONCLUSIONS

In this study, a classification-based post-compensation technique for color demosaicing is proposed. Based upon the interpolated result obtained from the former WM-HOI [9], the classification map is produced for the classified angle and variance of each pixel. All of the pixels belong to the same category which means that they have similar angle and variance, are trained to obtain a corresponding optimal filter. In post-compensation stage, the configuration of the angle and variance of each pixel determines the optimal filter for further reconstruction. Comparing to the original WM-HOI image, the simulation results demonstrate that the proposed scheme can improve the overall image quality, especially in the green plane, in particular, those regions of higher dynamic ranges. Notably, in fact the proposed CF-PCI scheme can be applied to any former schemes as a post-processing compensation and expectedly yields even better image quality.

#### ACKNOWLEDGEMENT

This work was supported by the National Science Council, Taiwan, under the Grants No. NSC100-2221-E-011-103-MY3 and No. NSC100-2221-E-182-047-MY3.

#### REFERENCES

- [1] B. E. Bayer, "Color Imaging Array," U.S. Patent 3 971 065, 1976.
- [2] T. Sakamoto, C. Nakanishi, and T. Hase, "Software pixel interpolation for digital still camera suitable for a 32-bit MCU," IEEE Trans. Consum. Electron., vol. 44, no. 4, pp. 1342-1352, Nov. 1998.
- [3] J. F. Hamilton and J. E. Adams, "Adaptive Color Plane Interpolation in Single Sensor Color Electronic Camera," U.S. Patent 5 629 734, 1997.
- [4] K.-H. Chung and Y.-H. Chan, "Color demosaicing using variance of color differences," IEEE Transactions on Image Processing, vol. 15, no. 10, pp. 2944-2955, Oct. 2006.
- [5] D. R. Cok, "Signal processing method and apparatus for producing interpolated chrominance values in a sampled color image signal," U.S. Patent 4 642 678, Feb. 10, 1986.
- [6] S.-C. Pei and I.-K. Tam, "Effective color interpolation in CCD color filter arrays using signal correlation," IEEE Trans. Circuits Syst. Video Technol., vol. 13, no. 6, pp. 503-513, June 2003.
- [7] J. S. J. Li and S. Randhawa, "High order extrapolation using Taylor series for color filter array demosaicing," in Springer Lecture Notes in Computer Science. New York: Springer, 2005, pp. 703-711, Series LNCS 3656.
- [8] J. S. J. Li and S. Randhawa, "Color filter array demosaicking using high-order interpolation techniques with a weighted median filter for sharp color edge preservation," IEEE Transactions on Image Processing, vol. 18, no. 9, pp. 1946-1957, Sep. 2009.
- [9] Widrow B. and Hoff M. E. Jr., "Adaptive Switch Circuits," IRE Western Electric Show and Convention Record, part 4, pp. 96-104, 1960. J. M. Guo and C. H. Chang, "Prediction-Based Watermarking Schemes Using Ahead/Post AC Prediction," Signal Processing, vol. 90, no. 8, pp. 2552-2566, August, 2010.
- [10] E. Kreyszig, Advanced Engineering Mathematics. New York: Wiley, 1999.
- [11] B. K. Gunturk, J. Glotzbach, Y. Altunbasak, R. W. Schaffer, and R. M. Mersereau, "Demosaicking: Color filter array interpolation," IEEE Signal Processing Mag., vol. 22, no. 1, pp. 44-54, Jan. 2005. H. M. Oh, C. W. Kim, Y. S. Han, and M.G. Kang, "Edge Adaptive Color Demosaicking Based on the Spatial Correlation of the Bayer Color Difference," EURASIP Journal on Image and Video Processing, No. 874364, 2010.
- [12] L. Zhang and X. Wu, "Color demosaicking via directional linear minimum mean square-error estimation," IEEE Transactions on Image Processing, vol. 14, no. 12, pp. 2167-2178, 2005.

[13] Magnus R. Hestenes, and Eduard Stiefel, "Methods of Conjugate Gradients for Solving Linear Systems," Journal of Research of the National Bureau of Standards, vol. 49, no. 6, pp. 409–432, 1952.  
 [14] <http://r0k.us/graphics/kodak/>

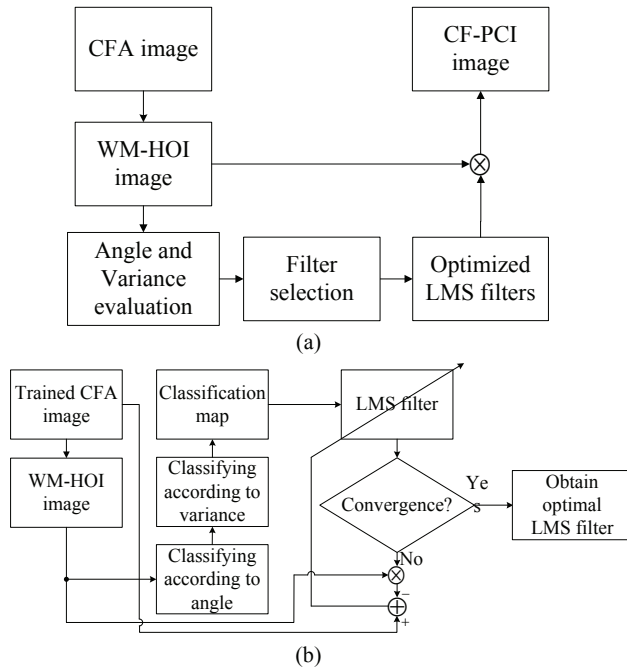


Fig. 1. Block diagram of the proposed CF-PCI algorithm. (a) Post-compensation scheme. (b) Off-line LMS training scheme.

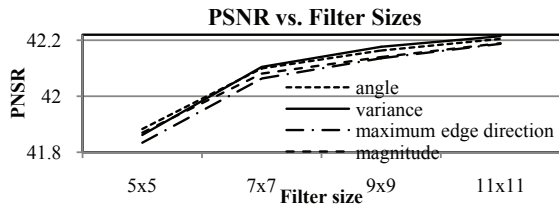


Fig. 2. Comparison diagram of the four features.

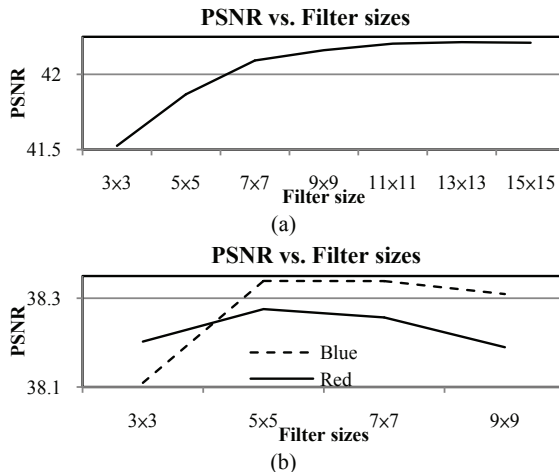


Fig. 3. Averaged image qualities under various LMS filter sizes. (a) Green plane. (b) Blue and red planes.

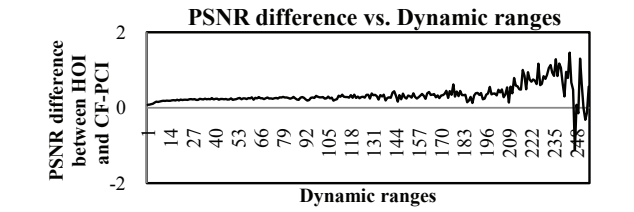
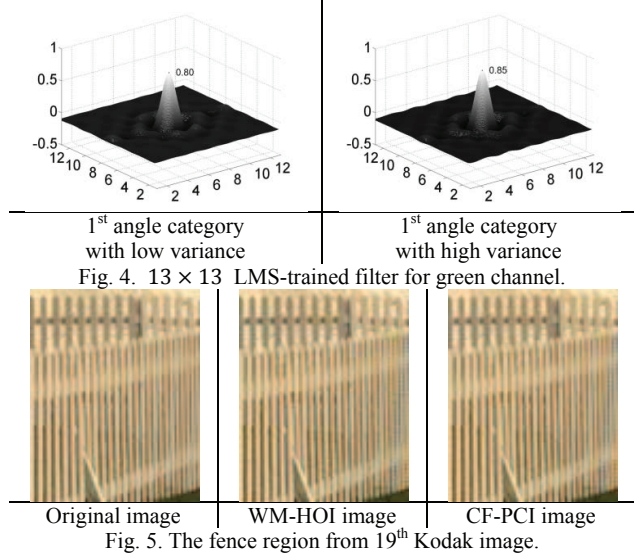


Fig. 6. PSNR different comparison chart between WM-HOI and CF-PCI of dynamic range on red and blue plane.

TABLE I IMAGE QUALITY COMPARISON BETWEEN THE RESULTS OF WM-HOI AND THE PROPOSED CF-PCI ALGORITHMS.

Kodak	Green (PSNR)		Red (PSNR)		Blue (PSNR)		Color (CPSNR)	
	WM HOI	CF-PCI	WM HOI	CF-PCI	WM HOI	CF-PCI	WM HOI	CF-PCI
13 <sup>th</sup>	34.15	35.53	33.83	33.87	32.51	32.68	33.44	33.88
14 <sup>th</sup>	38.65	39.83	35.31	35.49	35.99	36.25	36.43	36.82
15 <sup>th</sup>	41.48	43.17	36.22	36.50	39.88	40.27	38.66	39.14
16 <sup>th</sup>	42.55	44.56	41.26	41.55	40.57	41.00	41.38	42.12
17 <sup>th</sup>	41.92	42.89	40.67	40.92	39.78	40.28	40.82	41.23
18 <sup>th</sup>	37.42	39.06	35.47	35.57	35.89	36.02	36.18	36.63
19 <sup>th</sup>	40.14	41.89	38.21	38.30	38.75	39.22	38.96	39.56
20 <sup>th</sup>	41.84	43.57	40.54	40.97	37.92	37.95	39.83	40.24
21 <sup>th</sup>	39.02	40.86	38.09	38.32	36.78	37.15	37.87	38.52
22 <sup>th</sup>	39.57	40.79	37.10	37.45	36.65	36.86	37.60	38.06
23 <sup>th</sup>	44.17	45.74	39.83	40.15	39.58	39.74	40.84	41.16
24 <sup>th</sup>	36.16	37.38	34.40	34.87	32.39	32.45	34.05	34.32
Avg.	39.75	41.27	37.57	37.83	37.22	37.49	38.01	38.47